Proceedings World Geothermal Congress 2020+1
Reykjavik, Iceland, April - October 2021

Microwaving Graphene-Based Thermoset Polymers for Rapid and In-situ Wellbore Strengthening and Zonal Isolation

Rouzbeh Shahsavari

13000 Murpht Rd, Ste 102, Stafford, TX 77477, USA

Rouzbeh@ccretetech.com

Keywords: Microwave curing, wellbore strengthening, zonal isolation, graphene

ABSTRACT

The objective of this work is to develop a first-of-its-kind platform technology for in-situ and rapid wellbore strengthening as well as zonal isolation for geothermal wells such as EGS developments. Building on our recently elucidated scientific principles (https://doi.org/10.1021/acsami.6b01756), the core of our technology uses functionalized graphene nanoribbons (GNRs) embedded in suitable solutions (e.g. drilling fluids or high performance polymers), which will be irradiated with a microwave (MV) downhole tool for rapid curing. In drilling applications, the nanoscale functionalize GNRs dispersed in the drilling fluid will diffuse deep inside the rocks and dramatically enhance the mechanics of the entire rock via effective curing and reinforcement. In completion applications, the polymer solutions with GNRs break into crumpled (flexible) bags attached to a downhole tool, significantly expanding them to conformably cover the rough wellbore walls, followed by MV curing. In both applications, the functionalized GNRs act as electromagnetic antenna for efficient absorption of MV, and rapid and in-situ polymer curing. This platform technology allows effective prevention of wellbore instability on-the-fly as the drill bit advances, and also enables rapid and in-situ isolation of the multiple fracture zones, demonstrating a significant first-step in wellbore strengthening, sealing and zonal isolation for EGS and broader complex wells. This R&D combine the fundamentals of cutting-edge materials science, polymer chemistry, and advanced engineering followed by thorough testing in lab-simulated environments that are tailored to improve drilling efficiency and zonal isolations in openholes of EGS conditions.

1. INTRODUCTION

Along with tremendous incentives involved in extracting energy from renewable geothermal energy resources, significant challenges exist in developing new technologies to minimize cost and risk while maximizing the production. In this regard, wellbore strengthening and zonal isolation is one of the key problems facing EGS developments. The collapse of a wellbore during drilling and/or lack of an effective zonal isolation during completion (e.g. fracing) lead to significant difficulties such as reducing the rate of penetration, fluid leakage between the zones, and/or reduced stimulated pressure for fracing. These events will decrease the efficiency, capacity optimization, and economies of energy production from geothermal wells. In what follows, we focus on describing our technology and results for wellbore strengthening, and the extension to zonal isolation is essentially similar.

Wellbore reinforcement has received considerable attention over the last two decades since wellbore instability can lead to substantially higher drilling costs.[1,2] Microfractures present in the rock formation are a common cause of severe wellbore instability because drilling fluid seeps into these fractures thereby inhibiting the stabilizing effect of the drilling fluid overbalance and also reducing borehole pressure integrity by forcing fractures even further apart.[3-5] Therefore, there has been a great deal of effort to stabilize wellbores and prevent fluid loss by using additives such as mica, calcium carbonate, gilsonite and asphalt to seal microfractures.[6] However, these attempts have not been widely implemented since the size of conventional additives do not match that of the porous formation and they are far too slow in sealing microfractures. It is therefore recommended that deformable additives be developed with a broad size distribution capable of quickly sealing a wide-range of microfracture openings at an effective concentration that does not adversely affect the functional properties of the drilling fluid.[6]

Carbon nanomaterials have been used as additives for mechanical reinforcement of polymers and have recently shown that they penetrate through porous media.[7,8] Specifically, carbon nanotubes (CNTs) have been explored as polymeric reinforcements due to their small size, high Young's modulus, high tensile strength, and low percolation threshold.[9-15] Another remarkable property of CNTs is that they are highly efficient microwave absorbers.[16-20] Although the precise mechanism of CNT microwave interaction is poorly understood, nanotubes generate intense heat that could be used in a thermoset polymer for rapid curing at much lower microwave powers than those currently used in microwave assisted polymer curing (~900 W).[21-23] However, concerns over their toxicity as well as problems in preparing homogeneous CNT dispersions have plagued their commercial deployment.[24,25] Alternatively, graphene nanoribbons (GNRs), which are ribbon-like graphene made from chemically unzipping CNTs,[26] are now being considered for use as polymer reinforcements due to their remarkably low percolation threshold, high load transfer capability, and low toxicity.[27,28]

First, we show a proof of concept for wellbore strengthening by microwave heating functionalized GNRs dispersed in an oil based thermoset polymer to rapidly crosslink the matrix and thereby increase its mechanical resilience within sandstone. Polypropylene oxide (PPO) functionalization of the GNRs not only increased their dispersibility in the oil based drilling fluid, but also increased the amount of heat released by the GNRs under microwave irradiation, likely due to their superior dispersion. The temperature of the PPO-GNR polymer suspension dramatically increased above 200 °C within minutes under very low microwave power (30 W). The intense, localized heat from the PPO-GNRs cured the polymer within a short period of time producing both enhanced reinforcement and mechanical integrity of sandstone due to the improved load transfer characteristics from the microwave curing process. This method not only provides a simple and cost effective way to prepare polymer/carbon nanomaterial reinforced

composites, but also may be useful in extreme downhole conditions provided that there is a microwave source tool following the drill head.

2. RESULTS AND DISCUSSIONS

Our first goal was to synthesize GNRs that were soluble in an organic phase and aqueous phase, since both types of drilling fluids are used in industry. As prepared, GNRs have protons at the edges and showed poor dispersibility[32] in both water and Escaid™110 (a commercially available mineral oil based drilling fluid).[27] However, GNRs functionalized with PPO emanating from their edges showed good dispersion in both water (commonly used in geothermal wells) and Escaid™ 110 (Fig. 1a). Thermogravimetric analysis (TGA) showed gradual weight loss between 200-400 ºC due to the decomposition of PPO (Fig. 1b) thus confirming that 20% (20%-PPO-GNR) and 40% (40%-PPO-GNR) of PPO was functionalized on the GNR surface depending on the synthesis method. The presence of PPO was confirmed by Fourier transform infrared (FT-IR) analysis (Fig. 1c) with a characteristic peak at 2950 cm^{-1} indicative of C-H stretches. Raman spectroscopy (Fig. 1d) showed that the D/G ratios (0.48, 0.61, 0.84 for GNR, 20%-PPO-GNR, and 40%-PPO-GNR, respectively) increased with the amount of PPO functionalization due to the increased C-sp^3 content.

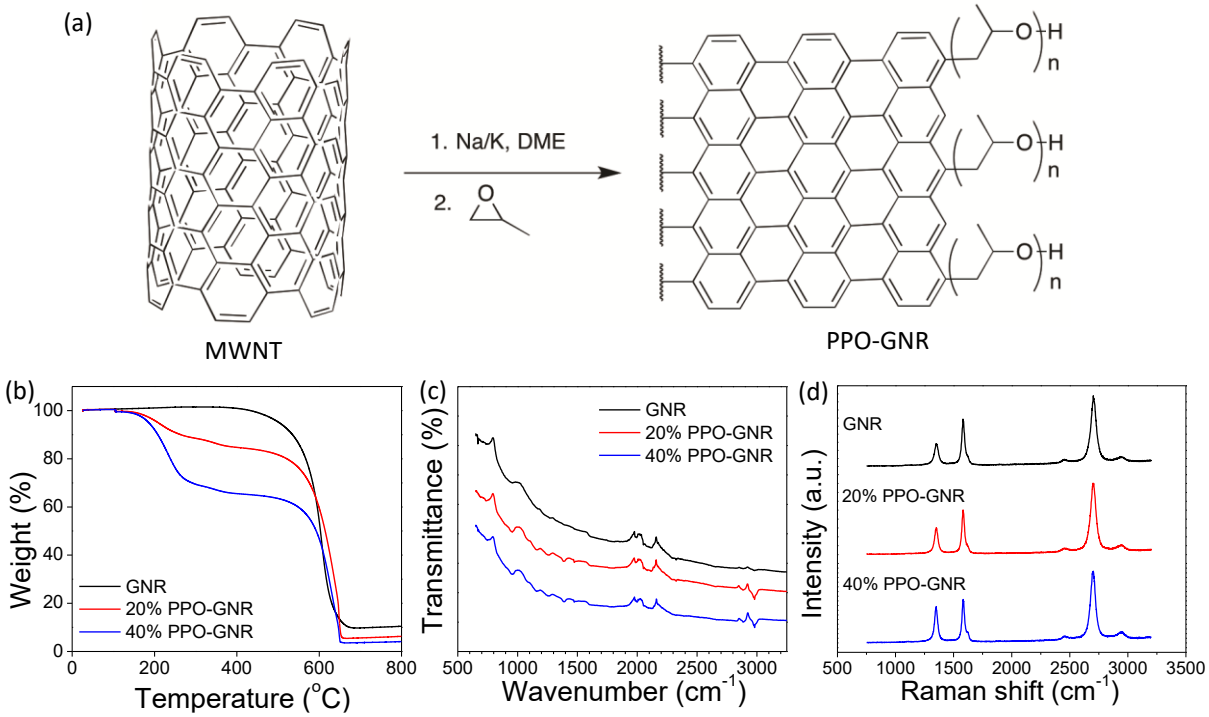

Figure 1. (a) Synthesis of PPO-GNRs from MWNTs. Only one tube within the MWNT is represented. Characterization of GNRs and PPO-GNRs by (b) TGA, (c) FT-IR, and (d) Raman.[32]

Before making a polymeric composite with PPO-GNRs, a suitable thermoset polymer should be selected that is readily available for curing at moderate temperatures. In addition, there are several criteria that must be considered in order to be an adequate thermoset polymer for downhole applications. First, polymerization needs to be done very quickly before fluid loss occurs thus reactive species are required. Second, the polymer should have a relatively high curing temperature to ensure that the high inherent temperature conditions in the wellbore do not prematurely result in crosslinking. Third, it must be inexpensive. And finally of low toxicity.

Given these selection criteria, as a starting point, we chose 1,2-polybutadiene (1,2-PBD) and ethylene glycol dimethacrylate (EGDMA) as the polymer backbone and crosslinking monomer, respectively (Fig. 2a). A cross linking polymer stock solution (Fig. 2b) was prepared by mixing 1,2-PBD/EGDMA into Escaid™110 which could then be heat cured in a 200 °C oven producing a rigid white polymer block. Differential scanning calorimetry (DSC) showed a sharp exothermic characteristic at 150 °C arising from its phase transition during curing (Fig. 2c).

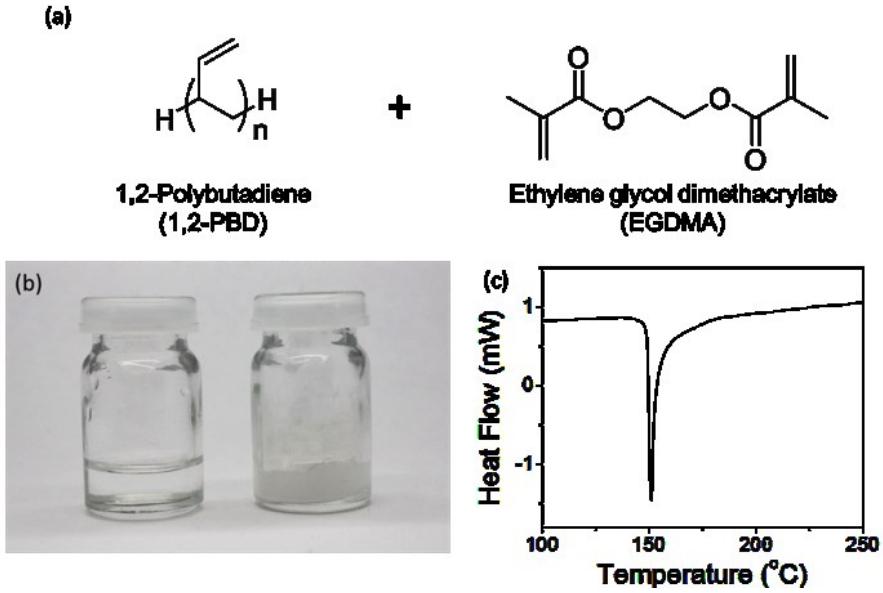

Figure 2. (a) Chemical structures of the polymer and crosslinker. (b) Image of the thermoset polymer stock solution before and after curing in an oven at 200 °C. (c) DSC characterization of the polymer solution.[32]

Fig. 3a illustrates the microwave waveguide and *in situ* temperature monitoring system used in our microwave assisted polymer curing experiments. Fig. 3b shows the heating profile of GNRs alone and PPO-GNRs with increasing amounts of PPO, but a fixed amount of GNRs (0.5 w/v%) in the polymer stock solution. The polymer/GNR suspension slowly heats under microwave exposure and did not increase in temperature to > 120 °C. However, PPO-GNRs show a much faster heating rate with an increase in temperature up to 200 °C within 10 min. 40%-PPO-GNR showed higher heating rates than 20%-PPO-GNR presumably due to the higher dispersibility in the oil-based polymer solution. However, extremely rapid heating and very high temperatures of the polymer may not be good for curing because it may decompose the polymer or induce excessive outgassing from the composite making it a porous structure. Therefore, further experiments were conducted using different amounts of 20%-PPO-GNR to optimize the process. The polymer stock solution itself did not display any significant microwave heating nor did the addition of a small amount of PPO-GNR (0.1 w/v%) significantly affect its heating rate (Fig. 3c). But since 1 w/v% of PPO-GNR heated rapidly to very high temperatures that could damage the polymer backbone, 0.5 w/v% of the 20%-PPO-GNR stock solution was selected for further mechanical testing.

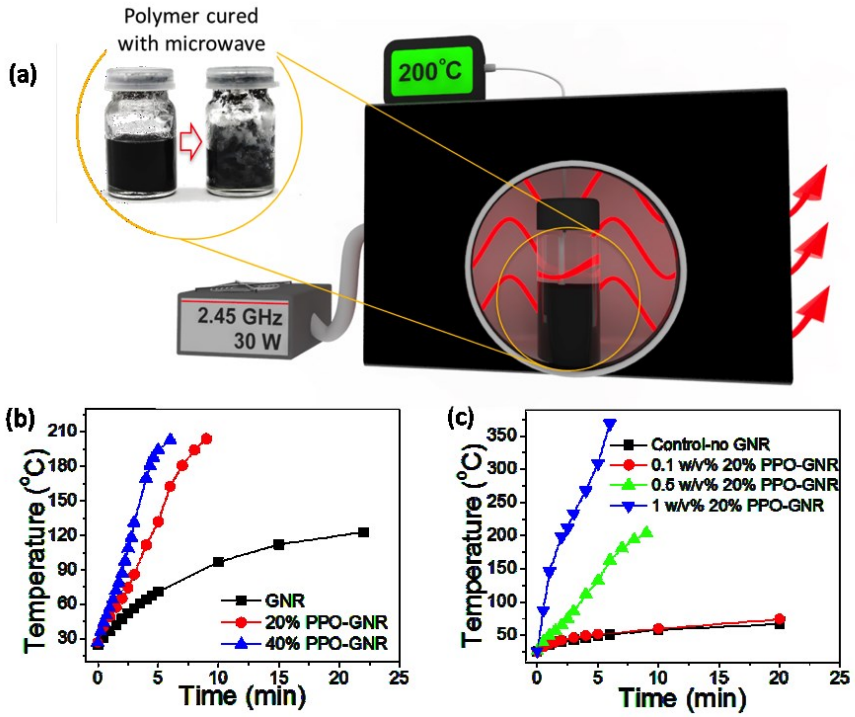

Figure 3. Microwave-assisted curing of polymer/PPO-GNR suspensions. (a) Illustration of the microwave-assisted polymer curing system using a waveguide and an *in situ* temperature monitor with a photograph of the polymer/PPO-GNRs suspension before and after microwave curing. (b) Microwave heating profile of GNR, 20%-PPO-GNR, and 40%-PPO-GNR suspensions. (c) Microwave heating profile of the polymer/PPO-GNR suspension containing different amounts of 20%-PPO-GNR.[32]

Fig. 4a schematically illustrates the process we used to infiltrate a block of porous sandstone with polymer/PPO-GNRs for microwave curing (SPG-M is designated for sandstone polymer-GNR microwave). Vacuum infiltration was used to drive the polymer/PPO-GNRs into the porous sandstone as a mimic for the pressured infiltration of a wellbore environment. A center cut section of the SPG-M showed numerous white spots that are not naturally present (Fig. 4b). Scanning electron microscopy (SEM) of SPG-M shows that the polymer and PPO-GNRs form thick film-like structures on the sandstone surface (Fig. 4c). In the cross-section of the SPG-M, we observed PPO-GNR strands attached onto the sandstone wall which confirms successful infiltration of the stock polymer/PPO-GNR solution (Fig. 4d). Elemental mapping of the sandstone using energy dispersive X-rays (EDX) shows the polymer and carbon nanomaterials were throughout the sandstone (Fig. 4e) as further confirmation that the sandstone and polymer composite structure had been successfully prepared.

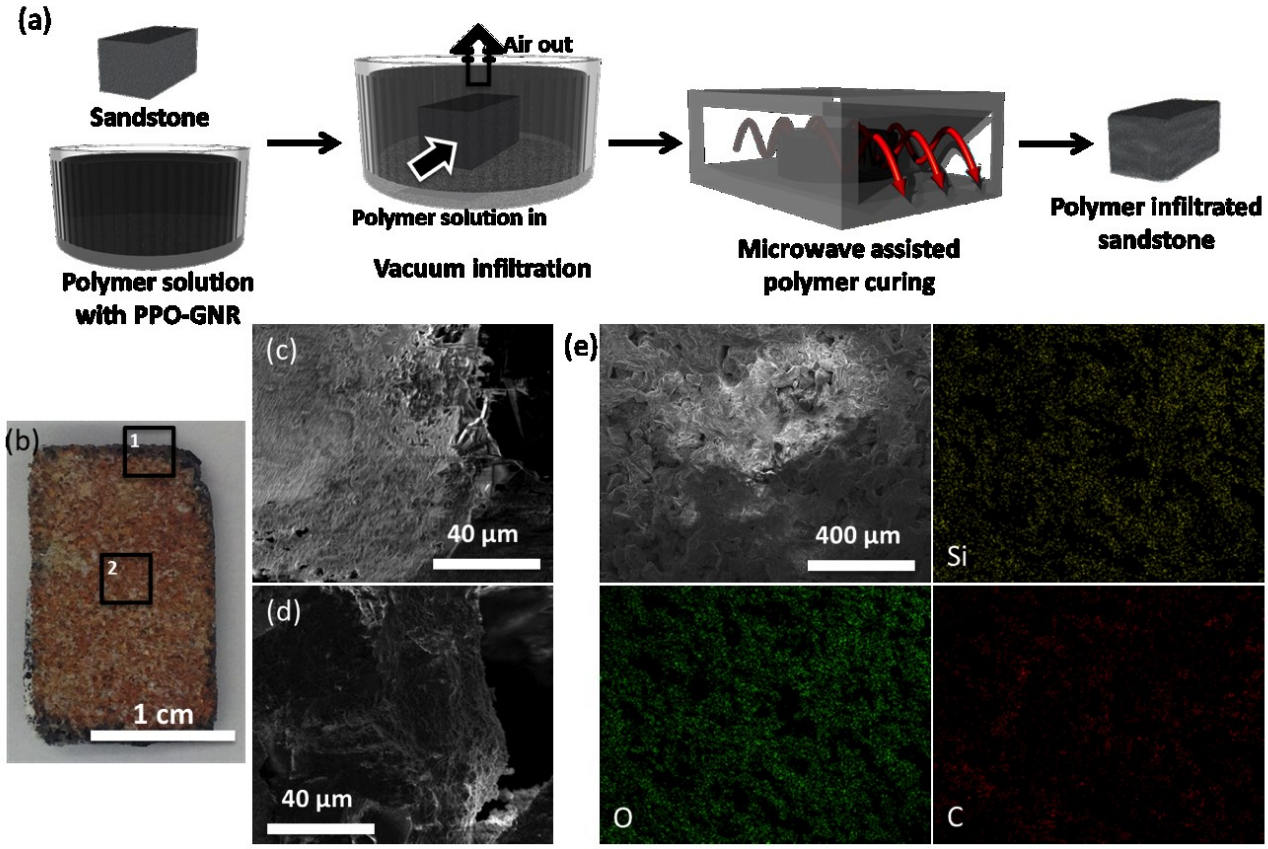

Figure 4. (a) Experimental scheme for preparation of microwave-cured polymer/PPO-GNR infiltrated sandstone (SPG-M). (b) Photograph of the cross-section of SPG-M. The black squares, 1 and 2, correspond to SEM images (c) and (d), respectively. (e) SEM image of the inside of SPG-M and corresponding EDX elemental mapping of Si, O, and C.[32]

Fig. 5 shows the ensemble mechanical properties from the compression experiments on the polymer-infiltrated sandstone. The compression system using the parallel bottom and top platens to apply uniaxial force develops a rather complex system of stresses due to the end restraints by the platens. However, due to Poisson's effect, the samples all undergo lateral expansion which results in creating cracks and eventually leads to failure of the samples. To compare the properties of SPG-M, several control samples were prepared using a convective oven to cure the materials. These control sandstone samples SP-O and SPG-O were cured in an oven without and with PPO-GNRs, respectively (O refers to oven-cured). By comparing these materials, the effect of either the addition of PPO-GNRs or microwave assisted polymer curing on the mechanical performance reinforcement was investigated.

Addition of polymer alone inside the sandstone increased the maximum compressive strength of the sandstone from 5.8 MPa to 8.4 MPa (Fig. 5a,b). This agrees well with the common intuition about such rock-type materials wherein the lower the porosity, the higher the compressive strength. However, with addition of PPO-GNRs, the maximum compressive strength of the SPG-M sample increased even higher to 11.3 MPa. Assuming equivalent porosities for oven cured sandstones infiltrated by polymer alone (SP-O) or polymer/PPO-GNRs (SPG-O), the ~35% increase in the compressive strength of SPG-O compared to SP-O is likely due to 1) the reinforcing effect of GNRs, which strengthen its surrounding matrix,[27] and 2) the high thermal conductivity of the GNRs, which causes more adequate and rapid curing of the polymer in SPG-O compared to SP-O, resulting in a more efficient high-strength adhesive bonding between polymer and sandstone. More impressive enhancement in reinforcement can be found in SPG-M, where the maximum compressive strength of SPG-M (13.3 MPa) increased more than 130 % compared to that of pure sandstone, and is even ~18% higher than that of SPG-O, the oven cured equivalent.

Such a strong reinforcement in SPG-M can be understood by comparing microwave assisted heating to convective heating of the polymer in SPG-O. In the oven-heated thermoset polymer, GNRs are just one part of a physical mixture inside the composite. Due to the low thermal diffusion through the sandstone and also through the non-uniformly distributed pores filled by polymer, heat cannot be homogeneously transferred to the GNRs dispersed in the polymer. However, with microwaves, each GNR absorbs

microwave energy independently and acts as a nanoscale heat generator with local temperatures that are high enough to thoroughly cure the surrounding polymer. Moreover, since the GNRs generate heat to induce polymerization, it can be assumed that the interface between the GNR and polymer has greater van der Waals interactions and will provide a more effective load transfer for stronger reinforcement than SPG-O. It could also be that the polymer chains added into the planes of the GNRs, but that was not confirmed here.

Furthermore, we know that GNRs toughen related polymers.[27,29] Here, the total toughness of the SPG-M (28.5 GPa) was ~1.6x higher than that of SPG-O, and also ~6x greater than that of pure sandstone (4.9 GPa) (Fig. 5c). Toughness is defined as the amount of energy a material absorbs before failure (representing the work-of-fracture), which is different from the classical "fracture toughness" with the unit of $P_a\sqrt{m}$. The work-of-fracture is the area under the stress–strain curve, which is deeply affected by gradual, "graceful fracture", whereas the fracture toughness does not incorporate this entire process.[9]

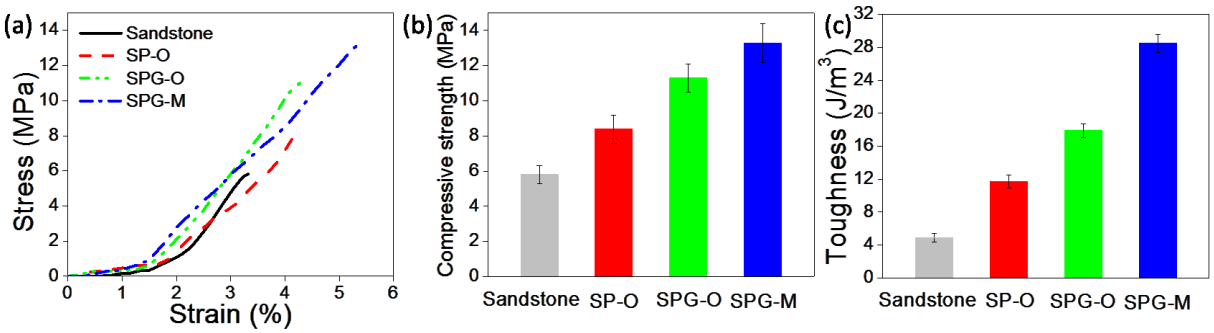

Figure 5. Compression mechanical tests of sandstone alone and polymer/PPO-GNRs infiltrated sandstones cured either by convective oven or microwaves. (a) Stress *vs* strain plot, (b) maximum compressive strength, and (c) toughness. Note: SP = sandstone infiltrated with polymer alone, SPG = sandstone infiltrated with polymer/PPO-GNRs, O = oven cured, and M = microwave cured.[32]

To investigate the micromechanics of the samples and to study the microstructural reinforcement effects of GNRs, a matrix-based algorithm was developed to conduct hundreds of indentations on the surface of the samples in order to directly obtain the mechanics of individual phases of the samples. The nanoindentation measurements were conducted by indenting 100 spots in a 10x10 matrix form using a Berkovich tip with a size of ~50 nm which allowed us to investigate the mechanical properties of the composite structure on both the nanometer and micrometer scales. Fig. 6a,b shows the surface of the SPG-M sample before indentation. Some imprints (triangles) of the indentation on the sample surface can be seen in Fig. 6c after unloading.

From the control experiments for the polymer and sandstone, the hardness value (which relates to strength) was found to be 30 MPa for the polymer alone, and over 1000 MPa for the sandstone alone (Fig. 6d inset). Therefore, to compare the mechanical reinforcement contribution of the polymer, hardness values larger than 1000 MPa were excluded from further analysis as they would correspond to the sandstone alone and not the cured polymer/PPO-GNRs. As GNRs were introduced to the polymer in the SPG-O, the hardness of the polymer was increased up to 180 MPa. However, for SPG-M, hardness values were > 200 MPa with values ranging from 200 to 900 MPa (Fig. 6d). The variation is due to the localized grid-like indented spots, which may or may not be in the vicinity of the GNRs. Nevertheless, the average hardness (~600 MPa) of all these spots in SPG-M is significantly higher than the average hardness of SPG-O (~100 MPa). Considering the measurement capabilities of nanoindentation (50 nm tip size and ~10 μm distance between the indentation spots), our results show the enhanced mechanical properties of SPG-M are mainly due to the strong-interaction between GNRs and the polymer, which improves the cross-linking and mechanical integrity of the polymer upon microwave irradiation. The elastic modulus of the samples was also calculated using the load-displacement curves (inset of Fig. 6e). All *P-h* curves in this figure showed smooth shapes and no pop-in behavior could be detected. The lower displacement of the SPG-M at the peak force indicates the higher hardness of this sample, compared to SPG-O/SP-O, resulting in lower material deformation. SPG-M also showed a highly enhanced elastic modulus compared to SPG-O owing to the incorporation of stiff GNR fillers into the polymer chains resulting in a stiffer composite material (Fig. 6e). These results indeed demonstrate that microwave assisted polymer curing in the presence of carbon nanomaterials can be a highly efficient for structural reinforcement. Lastly, further details of material preparations, testing and characterization procedures are given in reference 32.

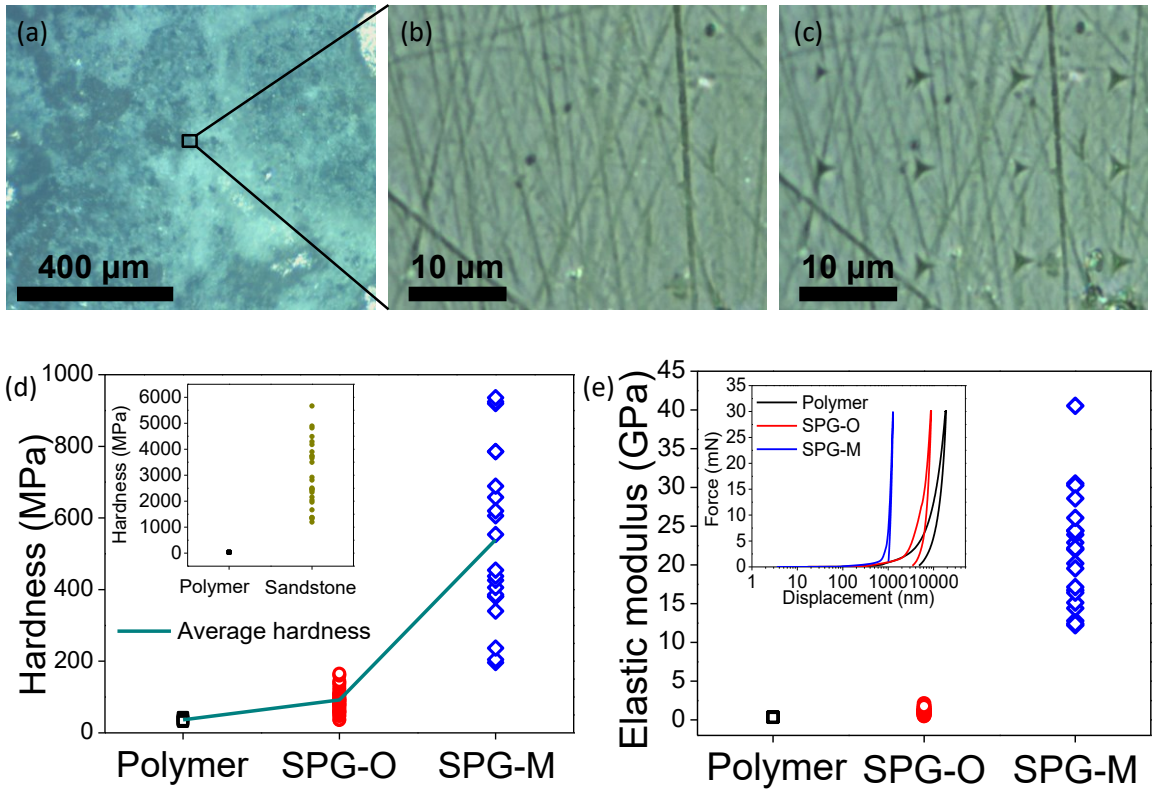

Figure 6. Nanoindentation test for the effect of microwave-assisted cured polymer on mechanical enhancement. (a) Optical image of the SPG-M sample before indentation experiments. Enlarged images (b) before and (c) after indentation. A part of the 10x10 matrix of indentation imprints (triangles) can be seen in (c). (d) Hardness values from nanoindentation experiments for polymer alone, SPG-O, and SPG-M. Inset shows difference of hardness between polymer and sandstone. (e) Elastic modulus value from the nanoindentation experiments for polymer, SPG-O, and SPG-M.[32]

3. CONCLUSIONS

In summary, we demonstrated that the use of GNRs as highly efficient fillers in polymers, combined with microwave-assisted localized heating, results in the significantly improved mechanical properties of polymer reinforced rocks. Systematic investigation of the mechanical properties (e.g. strength, toughness, and stiffness) of the polymer-reinforced sandstone at multiple length scales suggests that the interaction of carbon nanomaterials with a polymer matrix provides enhanced reinforcement even with a very low amount of carbon filler. Finally, while we showcased the benefits of this approach in the context of enhancing the mechanics of wellbore reinforcements, the concepts and strategies of this work, especially the use of low power microwave energy, can be easily applicable to a variety of rocks and extreme conditions of geothermal wells.

Further, we are currently applying a modified version of this technology for effective zonal isolation by creating effective high temperature tolerant polymer packers that will be cured rapidly via a microwave tool during completion stages. The technology will allow an entirely new phase space for highly efficient multistage zonal isolations with lower time and cost, significantly increasing the fracture predictability of stimulated fracture networks. The economic benefits are improved production (e.g. more productive reservoirs in less time, less money and lower number of wells), lower risk (e.g. seismic) and better use of EGS. Given the promises of staged stimulations to unlock the massive (100+ GW) capacity of EGS, this project will potentially lead to tremendous savings in cost and resources (water, personnel, equipment, etc.) in EGS development.

Acknowledgment: "This material is in part based upon work supported by the U.S. Department of Energy's Office of Energy Efficiency and Renewable Energy (EERE) under the Geothermal Technologies Office Zonal Isolation for Manmade Geothermal Reservoirs funding opportunity, Award Number DE-EE0008485."

REFERENCES

1. M. McLean and M. Addis, 1990, Presented at the 65th Annual Technical Conference and Exhibition, New Orleans, 23-26 October. SPE-20405-MS. DOI:10.2118/20405-MS

2. N. Morita and G.-F. Fuh, *SPE Drilling & Completion*, 2012, **27**, 315-327.

3. H. Wang, B. F. Towler and M. Y. Soliman, 2007, Presented at SPE/IADC Drilling Conference, Amsterdam, The Netherlands, 20-22 February. SPE-104947-MS. DOI:10.2118/104947-MS.

4. X. Chen, C. Tan and C. Detournay, 2002, Presented at SPE/ISRM Rock Mechanics Conference, Irving, Texas, 20-23 October. SPE-78241-MS. DOI:10.2118/78241-MS

5. R. Sweatman, S. Kelley and J. Heathman, 2001, Presented at SPE European Formation Damage Conference, The Hague, The Netherlands, 21-22 May. SPE-68946-MS. DOI:10.2118/68946-MS

6. F. Labenski, P. Reid and H. Santos, 2003, presented at SPE/IADC Middle East Drilling Technology Conference and Exhibition, Abu Dhabi, United Arab Emirates, 20-22 October. SPE-85304-MS. DOI:10.2118/85304-MS

7. J. M. Berlin, J. Yu, W. Lu, E. E. Walsh, L. Zhang, P. Zhang, W. Chen, A. T. Kan, M. S. Wong, M. B. Tomson, and J. M. Tour, *Energy Environ. Sci.*, 2011, **4**, 505-509.

8. C.-C. Hwang, L. Wang, W. Lu, G. Ruan, G. C. Kini, C. Xiang, E. L. Samuel, W. Shi, A. T. Kan, M. S. Wong, and J.M. Tour, *Energy Environ. Sci.*, 2012, **5**, 8304-8309.

9. N. Sakhavand and R. Shahsavari, *Nat. Commun.*, 2015, **6**, 6523.

10. H. Koerner, G. Price, N. A. Pearce, M. Alexander and R. A. Vaia, *Nat. Mater.*, 2004, **3**, 115-120.

11. S. Stankovich, D. A. Dikin, G. H. B. Dommett, K. M. Kohlhaas, E. J. Zimney, E. A. Stach, R. D. Piner, S. T. Nguyen and R. S. Ruoff, *Nature*, 2006, **442**, 282-286.

12. J. N. Coleman, U. Khan, W. J. Blau and Y. K. Gun'ko, *Carbon*, 2006, **44**, 1624-1652.

13. K. Lau, C. Gu and D. Hui, *Compos. Part B-Eng.*, 2006, **37**, 425-436.

14. Y. Li, K. Wang, J. Wei, Z. Gu, Z. Wang, J. Luo and D. Wu, *Carbon*, 2005, **43**, 31-35.

15. M.-F. Yu, O. Lourie, M. J. Dyer, K. Moloni, T. F. Kelly and R. S. Ruoff, *Science*, 2000, **287**, 637-640.

16. T. J. Imholt, C. A. Dyke, B. Hasslacher, J. M. Perez, D. W. Price, J. A. Roberts, J. B. Scott, A. Wadhawan, Z. Ye and J. M. Tour, *Chem. Mater.*, 2003, **15**, 3969-3970.

17. J. Kim, H.-M. So, N. Kim, J.-J. Kim and K. Kang, *Phys. Rev. B*, 2004, **70**, 153402.

18. K. R. Paton and A. H. Windle, *Carbon*, 2008, **46**, 1935-1941.

19. E. Vázquez and M. Prato, *ACS Nano*, 2009, **3**, 3819-3824.

20. Z. Ye, W. D. Deering, A. Krokhin and J. A. Roberts, *Phys. Rev. B*, 2006, **74**, 075425.

21. R. Bhandavat, W. Kuhn, E. Mansfield, J. Lehman and G. Singh, *ACS Appl. Mater. Interfaces*, 2012, **4**, 11-16.

22. A. L. Higginbotham, P. G. Moloney, M. C. Waid, J. G. Duque, C. Kittrell, H. K. Schmidt, J. J. Stephenson, S. Arepalli, L. L. Yowell and J. M. Tour, *Compos. Sci. Technol.*, 2008, **68**, 3087-3092.

23. V. K. Rangari, M. S. Bhuyan and S. Jeelani, *Compos. Part A-Appl. S.*, 2011, **42**, 849-858.

24. J. Du, S. Wang, H. You and X. Zhao, *Environ. Toxicol. Phar.*, 2013, **36**, 451-462.

25. X. Zhao and R. Liu, *Environ. Int.*, 2012, **40**, 244-255.

26. D. V. Kosynkin, A. L. Higginbotham, A. Sinitskii, J. R. Lomeda, A. Dimiev, B. K. Price and J. M. Tour, *Nature*, 2009, **458**, 872-876.

27. M. A. Rafiee, W. Lu, A. V. Thomas, A. Zandiatashbar, J. Rafiee, J. M. Tour and N. A. Koratkar, *ACS Nano*, 2010, **4**, 7415-7420.

28. M. Liu, C. Zhang, W. W. Tjiu, Z. Yang, W. Wang and T. Liu, *Polymer*, 2013, **54**, 3124-3130.

29. R. Nadiv, M. Shtein, M. Buzaglo, S. Peretz-Damari, A. Kovalchuk, T. Wang, J. M. Tour, and O. Regev, *Carbon*, 2016, **99**, 444-450.

30. B. Genorio, W. Lu, A. M. Dimiev, Y. Zhu, A.-R.O. Raji, B. Novosel, L. B. Alemany, and J. M. Tour, *ACS Nano*, 2012, **6**, 4231-4240.

31. R. Shahsavari and F.-J. Ulm, *J. Mech. Mater. Struct.*, 2009, 4, 523-550.

32. N. Kim, A. Metzler, V. Hejazi, A. Kovalchuck, S.K. Lee, R. Ye, J. Mann, C. Kittrel, R. Shahsavari, J. Tour, Microwave Heating of Functionalized Graphene Nanoribbons in Thermoset Polymers for Wellbore Reinforcement, *ACS Appl. Mater. Inter.* 2016, **8**, 12985-12991.